Mode Recovery of Multi-component Signal using Synchrosqueezing Transform

Adarsh Akkshai Venkataramani* and Vineet Sunil Gattani†

Abstract

The goal of this project is multi-component signal reconstruction using time-frequency(TF) representations. To this end, we choose a post-processing transform called the Synchrosqueezing Transform(SST). SST circumvents the uncertainty relation inherent to linear transforms, such as the Short Time Fourier Transform(STFT) by reassigning the coefficients along frequency axis. This reassignment results in a sharper TF representation and also maintains the invertibility of the operator. We explore the limits of this transform on both TF representation and signal recovery. The researchers have theorized and discussed some initial results by making the mode recovery process optimal and adaptive in nature.

1 Introduction

A wide class of naturally occurring signals can be described by the superposition of amplitude and frequency modulated (AM - FM) modes. These signals are formally called as multicomponent signals(MCS).

$$x(t) = \sum_{k=1}^{K} x_k(t), \quad \text{with } x_k(t) = A_k(t)e^{i\phi_k(t)} \tag{1}$$

where the kth mode of the signal, $k = 1, \ldots, K$, $A_k(t)$, $\phi_k(t)$ are the time dependent amplitude and phase, respectively. The problem of resolving the modes of $x(t)$ is non-trivial and an active field of study. Broadly there are two scopes of study, either the localized representation of signals in the time-frequency plane and the recovery of the MCS modes. This paper explores the feasibility of recovery

1.1 Background

Time-frequency representations can be visualized as physical densities of frequency components of a time varying signal $x(t)$. Analogous to the representation of momentum and position of particles they share the uncertainty principle of Heisenberg and as a consequence they are inherently limited in resolution, $\Delta t \Delta f \geq$

*Researcher 1
†Researcher 2

$\frac{1}{4\pi}$. Post-processing techniques assist in TF localization, by using techniques such as reassignment, smoothing kernels on ambiguity functions [1] etc. Such post-processing techniques operate on various time frequency representations from different classes, ex: Cohen's class, Hyperbolic Class, Affine class etc. This study is restrictive to Cohen's class linear time-frequency representations. In contrast to quadratic representations such as the Wigner-Ville Distribution(WVD), they enjoy simplistic representation, independence to blurring cross terms and preserve time and frequency shifts. In addition to maintaining time and frequency shifts and other properties which can be viewed in [2]. A very common linear TFR used in most applications is the Short Term Fourier Transform(STFT). STFT uses a constant window in time to analyze frequency components, recalling the 1-D Fourier transform we understand there is a spread caused due to the window. An application of the post-processing technique such as reassignment on the magnitude of this STFT would permit good resolution in frequency.

Section 2.3 discusses the reassignment technique in detail, deriving the center of gravity for time and frequency. The reassignment performs along both the time and frequency axis. The reassigned spectrogram facilitates for an enhanced time-frequency representation, since spectrogram is the magnitude of the STFT, direct recovery from the spectrogram would be impossible. Soon thereafter reassignment technique was sidelined until recently it resurfaced in a different framework which allowed signal reconstruction. Maes and Daubechies developed a phase based techniques called the Synchrosqueezing [3], which is a special case of the reassignment method. This technique was developed for the Continuous Wavelet Transform (CWT) and was later extended to the STFT [4],[5] as Fourier based Synchrosqueezing Transform(FSST). The FSST will be discussed in depth in Section 3. The FSST was developed under certain set of assumptions which will be discussed in depth in the sections to come.

FSST is advantageous as it enables one to separately represent modulated or closely spaced signals with higher resolution to the STFT. This permits us to use the ridge signatures estimated from time-frequency representations using ridge extraction. For this, there are a significant number of methods that exists. The ridge extraction techniques will be discussed in Section 5. Signal recovery and reconstruction accuracy is essential to understand given the number of total modes. Sections 6.2, 6.4 are used to discuss the importance of the frequency separation and the ideal number of frequency bins required to clearly isolate two signals.

2 Short review on known techniques

2.1 Short Time Fourier Transform

Given a signal $x(t)$ such that it exists with a finite support in $\mathcal{R}$. The generalized notation of the STFT of a time varying signal with a window $h(t)$ of finite length is given as:

$$S_x^g(t,f) = \int_{\mathcal{R}} x(\tau)h(\tau - t)e^{-2i\pi f\tau}d\tau \tag{2}$$

The resolution and the localization in the time frequency domain is determined by the length of the window. As discussed in Section 1, the linear TFR, here the STFT is bound by the uncertainty principle. In general, increasing the length of the window in the time domain increases the frequency resolution of the time-frequency representation.

2.2 Window parameters

We have chosen a Schwartz class window, Gaussian window $h(t)$ defined by

$$h(t) = e^{(-\frac{\pi t^2}{\sigma^2})} \tag{3}$$

where σ is the standard deviation of the Gaussian window and its value is set to 0.035, with the frequency bandwidth/support set as 34Hz. For sake of brevity, we analyze all signals using only this window size, the reasoning of choosing this constant window length can be found in 3.1, from hereon all windows will be subscripted as g or recalled as $g(t)$.

2.3 Reassignment technique

Reassignment is a contemporary technique of pruning time frequency localization of the *spectrogram* $|S_x^g(t,f)|^2$, for a signal x and moving window h. The spirit of the idea is to centralize the distribution of energy in the TF plane, caused due to window effect of the STFT. The idea is to find a primary center, analogous to the idea of calculating the center of mass of an object, and immediately mapping all distribution of the mass to occupy a finite point with maximum density [1], or a more observable military drill, where all disoriented army personnel jump back into a straight line. Projection of the distribution to a finite density point, requires calculation of the centroid of the signal. This centroid is obtained from the phase of the STFT as:

$$\hat{t}_x(t,\omega) = \frac{t}{2} - \partial_\omega\phi(t,\omega) \tag{4}$$

$$\hat{\omega}_x(t,\omega) = \frac{\omega}{2} + \partial_t \phi(t,\omega) \tag{5}$$

where $\partial_\omega \phi(t,\omega)$ is the derivative of phase of STFT with respect to ω, and $\hat{t}$ and $\hat{\omega}$ are the. group delay(GD) and the local instantaneous frequency(IF) of the analyzed signal.

The reassigned spectrogram is then defined as:

$$\hat{S}_x^g(t,\omega) := \int\int_{\mathcal{R}} S_x^g(s,\kappa)\delta(t - \hat{t}_x(s,\kappa), \omega - \hat{\omega}_x(s,\kappa))\frac{dsd\kappa}{2\pi} \tag{6}$$

This is valid as long as the signal is the time variation is slow relative to the phase variation.

3 Synchrosqueezing Transform

The Synchrosqueezing Transform(SST) performs an operation of frequency reassignment directly on the STFT. It can be viewed as a post-processing operation when provided with the STFT of a signal $x(t)$. It is of particular interest to note the local derivative(IF) of the signal can be used to represent the ideal TFR around the local region $\mathcal{S}$, $\mathcal{S} \subset \mathcal{R}$, and is useful to understand the complete phase of the signal.

As discussed in 2.3 we estimate the local IF by computing the centroid $\hat{\omega}_x(t,f)$. Using a similar idea as reassignment it follows that the SST operator reassigns the STFT as:

$$T_x(t,\omega) = \frac{1}{g(0)}\int_R S_x^g(t,\nu)e^{i\omega t}\delta(\omega - \hat{\omega}_x(t,\nu))d\nu \tag{7}$$

where $S_x^g(t,\nu)$ is the computed STFT of the input signal $x(t)$ using a window $g(t)$. $\hat{\omega}_x(t,\nu)$ is the centroid calculated along the frequency axis. Immediate observation of 7, shows it's closeness to the reassignment technique. The value of $\hat{\omega}_x(t,\nu)$ is computed in an efficient mathematical framework which will be discussed in Section 3.2. This operator performs reasonably for a set of weakly modulated MCS AM-FM signals, as discussed in the next section.

3.1 Mathematical assumptions of SST

For the class of signals given in 1, we have a set $\beta_{\Delta,\varepsilon}$ in the class of MCS, which satisfies the following criteria, $A_k(t) \in L^\infty$, $\phi_k(t) \in L^\infty$, $A_k(t) > 0$, $\phi_k'(t) > 0$, $|A_k'(t)| \leq \varepsilon$ and $\phi_k''(t) \leq \varepsilon$, such set of signals belong to the family of weakly modulated signals. The frequency bandwidth of the window lies in $[-\Delta, \Delta]$, since the window is Gaussian, a Schwartz class window, $\Delta = \frac{\sqrt{(2\log(2))}}{\sigma}$. We may represent the lower bound of isolation of frequencies as:

$$\inf_{t} \quad \phi'_k(t) - \sup_{t} \quad \phi'_{k-1}(t) \geq 2\Delta \tag{8}$$

which corresponds to the clear isolation of modes in frequency. Lastly, We always are aware of the number of modes present in the MCS signal.

3.2 Computing the centroid $\hat{\omega}_x(t, \omega)$

The SST operator moves the coefficients of the STFT from (t, ω) to $(t, \hat{\omega}_x(t, \omega))$. Extending the equation 5, the computation of the local instantaneous frequency $\hat{\omega}_x(t, \omega)$ can be theoretically defined as:

$$\hat{\omega}_x(t, \omega) = \frac{1}{2\pi} \arg S_x^g(t, \omega) \tag{9}$$

In order to compute the frequency reassignment operator $\hat{\omega}_x(t, \omega)$, the partial derivative of the phase were replaced by:

$$\hat{\omega}_x(t, \omega) = \omega - \Im\left\{ \frac{S_x^{dg}(t, \omega)}{S_x^g(t, \omega)} \right\} \tag{10}$$

where $\Im\{M\}$ is the imaginary part of the complex number M. $S_x^{dg}(t, \omega)$ stands for the STFT of the input signal $x(t)$ computed with the derivative of the analysis window $dg(t) = \frac{dg(t)}{dt}$. Given an analysis window $g(t)$ one can compute a good approximation of the derivative of the window by taking the first order difference of its coefficients. Therefore, the centroid $\hat{\omega}_x(t, \omega)$ can be calculated efficiently using just two STFTs.

Following from the hypotheses of clear isolation 3.1, one can understand that for any (t, ω) there exists an error in the estimate of IF, $|\hat{\omega_x}(t, \omega) - \phi'_k(t)| \leq C\epsilon$, where C is some constant and $\epsilon > 0$.

4 Simulation of time-frequency representation

Our experimentation is three-fold, we first consider synthetic signals with clearly known modes, we then experiment SST on a real world application such as a sonar signal.

4.1 Synthetic signals

For our first simulation, we create a synthetic signal $s_1(t)$containing 3 modes. The three modes are defined as:

$$\begin{cases} x_1(t) = e^{(8(t-1/2*4096)^2)} \sin(2\pi(250t + 100t^3)) \\ x_2(t) = e^{(8(t-1/2*4096)^2)} \sin(2\pi(130t + 100t^2)) \\ x_3(t) = e^{(8(t-1/2*4096)^2)} \sin(2\pi(90t + 0.2cos(3\pi t))) \\ s_1(t) = x_1(t) + x_2(t) + x_3(t) \end{cases} \tag{11}$$

where $s_1(t)$ consists of a sinusoid of constant frequency 90Hz, a linear chirp with frequency ranging from $[130, 330]$ Hz and a quadratic chirp with frequency ranging from $[250, 550]$ Hz. The duration of the signal is 1 second and the sampling frequency is 4.096 kHz.

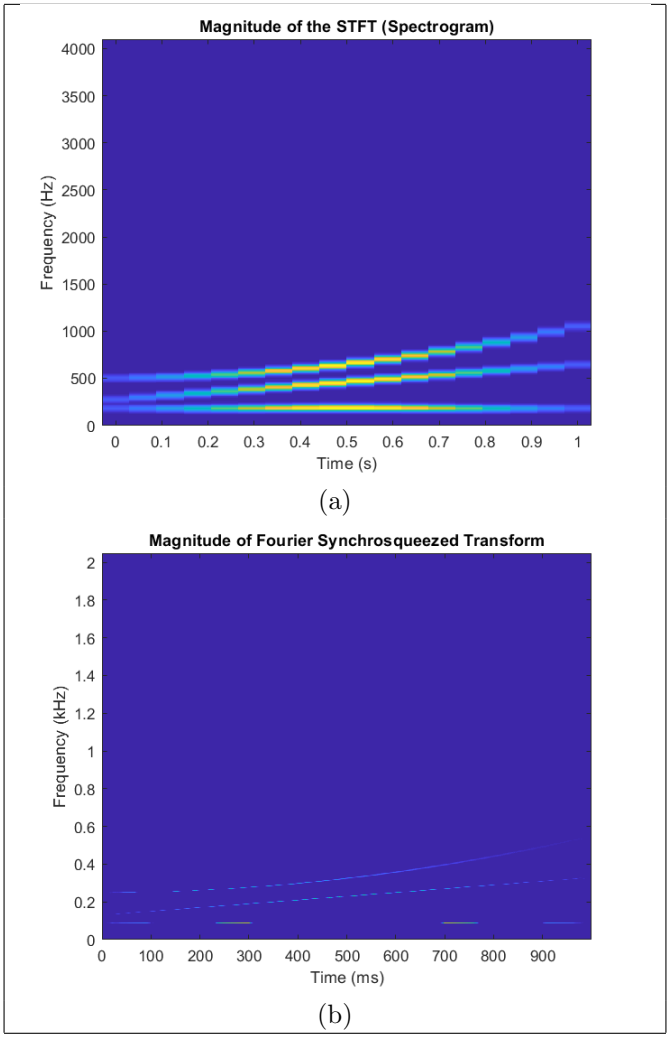

Figure 1: TF representations of $s_1(t)$ (a) Spectrogram (b) Fourier based Synchrosqueezing, window length is as discussed in 2.2

.

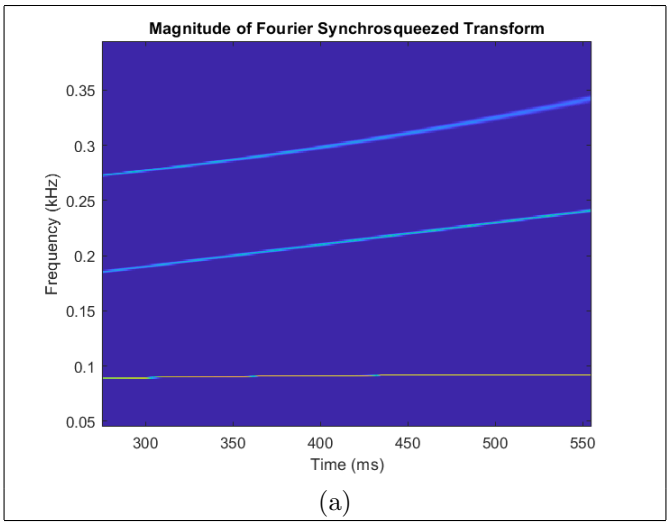

(a)

Figure 2: Zoomed SST representation of $s_1(t)$ for a smaller but finite time interval.

.

4.2 Faulty gearbox simulation

For our second simulations, we take the example from [9] of a simulated vibration signal $s_2(t)$ of a faulty gearbox with variable speed. The mathematical form of such a signal is given by

$$\begin{cases} p_1(t) = cos(50\pi(3t + 5t^2 - 2t^3) + 2.5sin(0.6\pi t)) \\ p_2(t) = 0.5cos(60\pi(3t + 5t^2 - 2t^3) + 2.5sin(0.6\pi t)) \\ p_3(t) = 0.5cos(40\pi(3t + 5t^2 - 2t^3) + 2.5sin(0.6\pi t)) \\ s_2(t) = p_1(t) + p_2(t) + p_3(t); \end{cases} \tag{12}$$

The duration of the signal is 1 second and the sampling frequency is 4.096 kHz.

4.3 Bat echolocation signal

This signal is taken from MATLAB which is an echolocation pulse emitted by a big brown bat (Eptesicus Fuscus). The sampling interval is 7 microseconds.

5 Ridge extraction

A ridge can be defined in a very general setting as the projection of a surface $Q = f(x, y)$ onto a (x, y) plane. The ridge set R can be defined as the set of local maxima in frequency plane. The assumption is the set R consists of k ridges for each mode and it is always connected over the domain of the signal in TF

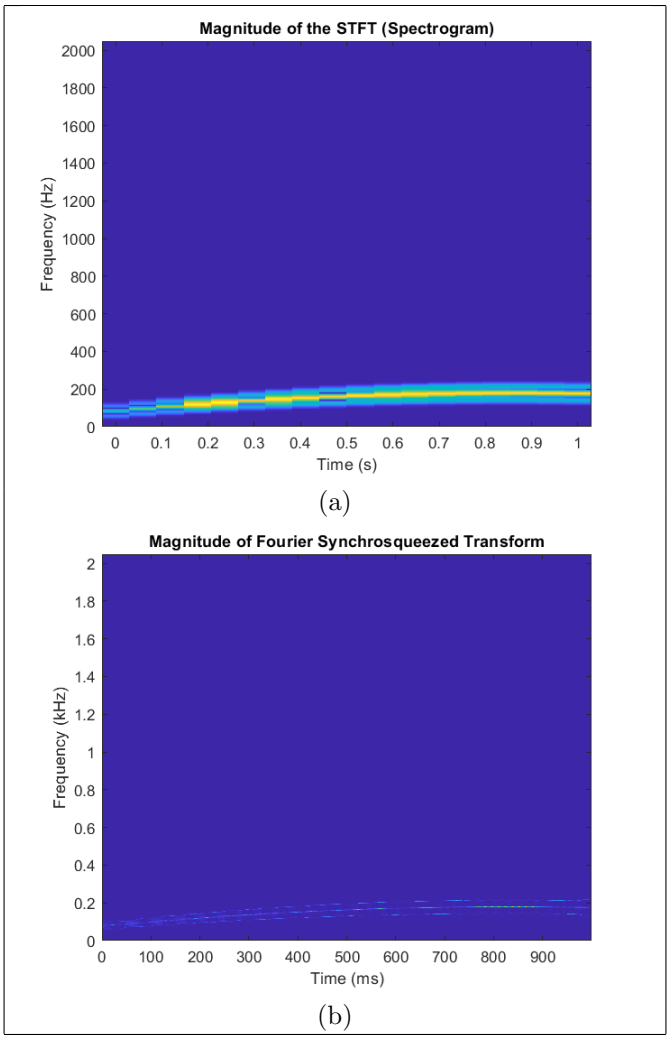

Figure 3: TF representations of $s_2(t)$ (a) Spectrogram (b) Fourier based Synchrosqueezing, window length is as discussed in 2.2

.

plane, in addition we also impose that the ridges are not intersecting, since the ridges will not adhere to the true nature of the signal. We may assume the ridge map to be an IF map for the sake of representation. There are numerous methods for extraction of ridges, from penalization methods to active snakes and other methods [8]. Each of these methods present their own advantage which is discussed elaborated in [8]. Most methods involve maximization of the energy functional from [4]:

$$E_x(\omega) = \sum_{k=1}^{N} - \int_{\mathcal{R}} |T_x^g(t,\omega)|^2 dt + \int_{\mathcal{R}} \lambda \phi_k'(t)^2 dt + \int_{\mathcal{R}} \beta \phi_k''(t)^2 dt \tag{13}$$

They assert the formulation is appealing in mathematical sense while its implementation is hard in

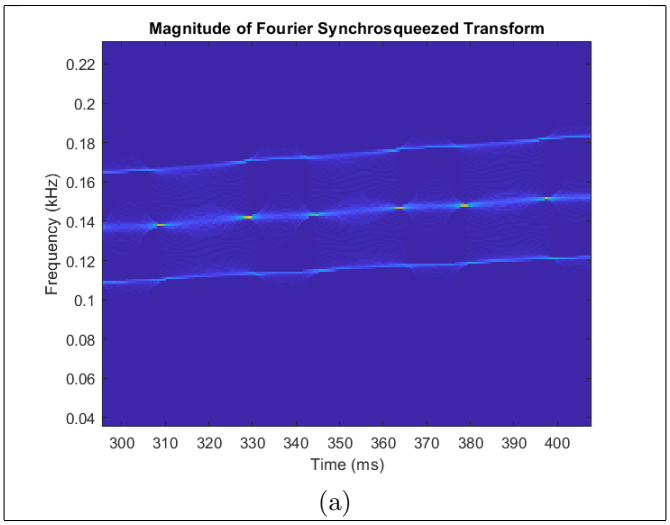

(a)

Figure 4: Zoomed SST representation of $s_2(t)$ for a smaller but finite time interval.

.

practice and a requires heuristic algorithm such as simulated annealing or random walks. Random walks are efficient in case of noisy contexts and easy to use. Considering the trade-offs we choose to proceed using 'Crazy Climber Detection Algorithm', at it's core it's a Markov Chain Monte Carlo Method (MCMC). This type of Monte Carlo methods encourages to initiate random points and to make tentative steps around an area to make reasonable contribution towards reaching the local maxima. Our case uses a Hastings-Metropolis penalization to reject bad decisions and promote faster 'climbs'.

5.1 Crazy Climbers

Algorithm 1 Crazy Climbers Algorithm

Obtain TF representation $X(t, \omega)$
Initialize $k = 0$
$p \sim \{\frac{1}{2}, \frac{1}{2}\}$
$q \sim \{\exp(\Delta M/T(t_k)), 1 - exp(\Delta M/T(t_k))\}$
Initiate N climbers on TF grid $X(t_k, \omega_k)$, $t \in (0, K)$ and $\omega \in (0, B)$
while $t_k < K$ **do**
  if $p\{t_k\} = \frac{1}{2}$ **then**
    $t_k = t_k + 1$
  else
    $t_k = t_k - 1$
  end if
  Begin Vertical search on the TF grid
  if $\Delta M = X(t_k, \omega_k) - X(t_k, \omega_{k-1}) \geq 0$ **then**
    $q\{\omega_k\} = \omega_k + 1$
  else
    $q\{\omega_k\} = \omega_k - 1$
  end if
end while

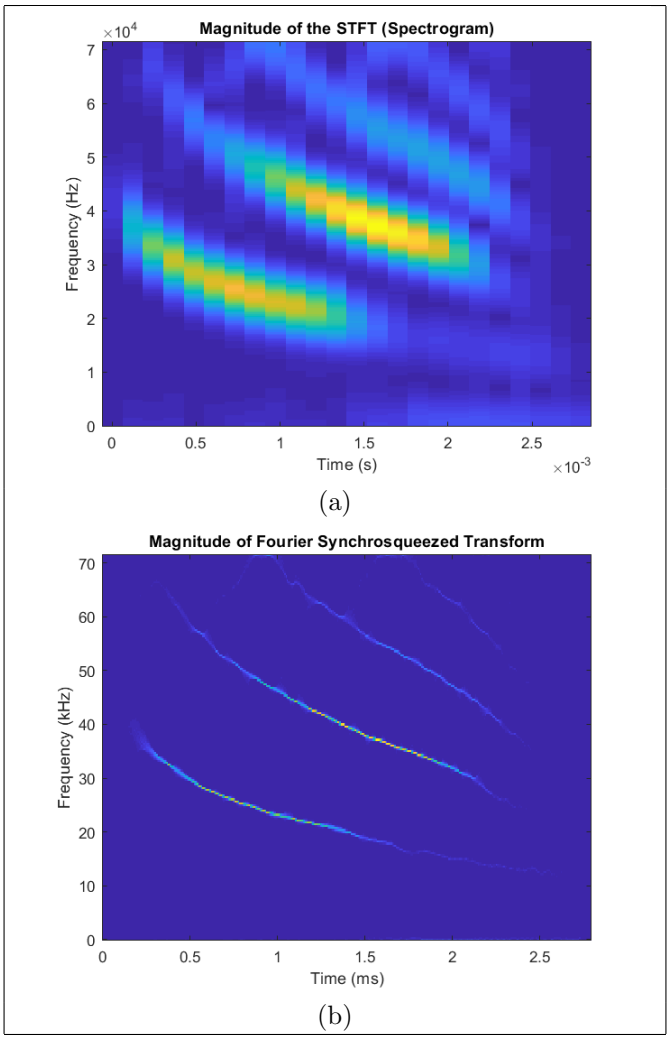

Figure 5: TF representations of bat signal from **batsignal.mat** (a) Spectrogram (b) Fourier based Synchrosqueezing, window length is as discussed in 2.2

.

After a finite number of ridges are measured, an occupational criterion weighs every climber necessary for highly accurate ridges.

6 Signal Recovery Strategies

6.1 Direct

The reconstruction of a signal $x(t)$, can be related to the synthesis equation:

$$x(t) = \frac{1}{2\pi g(0)} \int_{\mathcal{R}} S_x^g(t,\omega) e^{i\omega t} d\omega \tag{14}$$

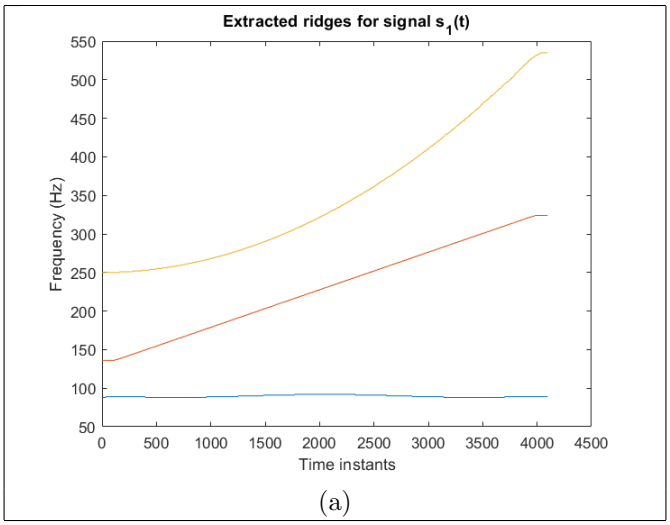

(a)

Figure 6: Ridge extraction of a 3 mode signal $s_1(t)$, having close resemblance to the ideal TF representation, the number of extracted ridges are 3

Since the STFT $S_x^g(t,\omega)$, is invertible we get back the reconstructed signal from the above equation 14. The SST operator is the frequency reassigned version of the STFT, it still maintains it's invertibility property. Therefore one can reconstruct the original signal using the SST operator as follows:

$$x(t) = \frac{1}{2\pi g(0)} \int_{\mathcal{R}} T_x^g(t,\omega) e^{i\omega t} d\omega \tag{15}$$

where $T_x^g(t,\omega)$ is the SST operator.

6.2 Individual mode recovery

After computing the SST operator $T_x^g(t,\omega)$, the k^{th} mode can be reconstructed in the surroundings of its estimated ridge.

$$x_k(t) \approx \int_{\{\omega, |\omega - \Phi_k(t)| < d\}} T_x^g(t,\omega) e^{i\omega t} d\omega \tag{16}$$

where d is defined as the time-frequency support of the ridge.

6.3 Signal reconstruction

6.4 Varying the parameter d

The above signal reconstructions were performed based on a constant frequency support d defined in Section 2.1. To recall it is 34Hz. It is of interest to vary the length of the support and observe the reconstruction performance. One can intuitively say that a support that spans a huge frequency bandwidth could yield

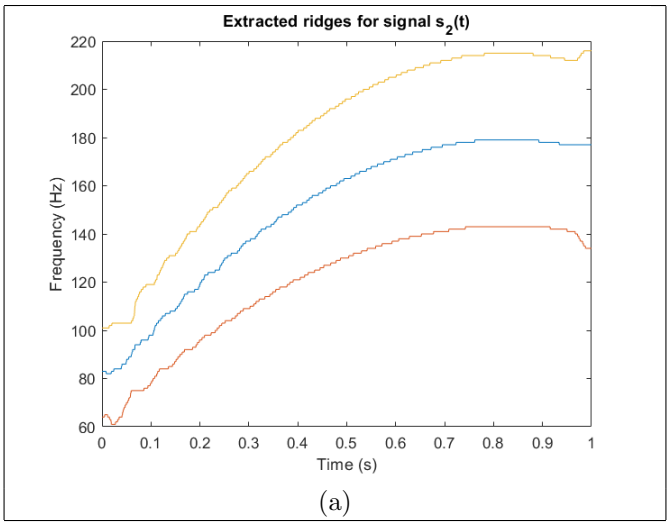

(a)

Figure 7: Ridge extraction of a 3 mode signal $s_2(t)$, having close resemblance to the ideal TF representation, number of extracted ridges are 3

better reconstruction of the signal if the modes the support for the current ridge does not overlap with the ridges around it. The d parameter must satisfy the following inequality condition

$$d \leq \begin{cases} \Phi_{k+1}(t) - \Phi_k(t) \\ \Phi_k(t) - \Phi_{k-1}(t) \end{cases} \tag{17}$$

where $\Phi_k(t)$ is ridge of the k^{th} mode. In practicality, the time-frequency support is the number of frequency bins we select around a corresponding ridge.

7 Discussion of results

From the theoretical study of SST in Section 2.1 and 3, the reassignment operator provides an enhanced TFR. We have first considered a case of generating a synthetic signal with well separated modes in the time-frequency plane. Fig. 1 show the spectrogram and the synchrosqueezing transform of the signal $s_1(t)$. A constant Gaussian window in time domain is used for the computation of the spectrogram and the SST. The synchrosqueezed transform of the $s_2(t)$ displayed in Fig. 3 has a sharper representation when compared to the spectrogram representation of the same signal. The time-frequency representaion of the SST shows perfect localization of time and frequency. To generalize the notion of sharper and enhanced TFR provided by the SST we perform the synchrosqueezing on a signal studied in [9]. The signal represents the simulation of the vibration signal of a faulty gearbox. The modes in this signal are closely packed. The spectrogram for this signal $s_2(t)$ is barely able to resolve the three modes using the specified window in Section 2.1. On

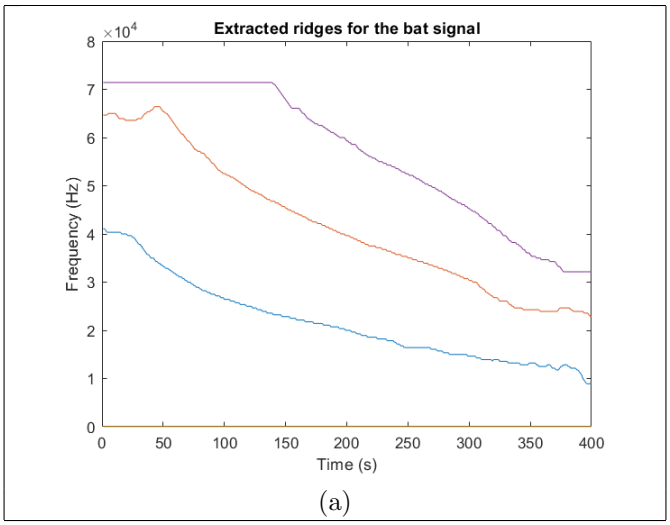

(a)

Figure 8: Ridges extracted from the SST operator computed for the bat signal. The number of extracted ridges are 4.

the other hand the SST givens a clear mode separation. To test the limits of SST, we have then performed the SST operation on a bat echolocation signal taken from MATLAB. It consists of four distinct hyperbolic chirps. Fig. 5 shows the results of the spectrogram plot and the synchrosqueezed plot of the bat signal. It is clear from all the above comparisons that the synchrosqueezing provides a visually appealing and distinct separation of modes of a given signal.

Given the computed SSTs from the given signals we proceed towards ridge extraction. Considering the signal $s_1(t)$ and performing the ridge extraction on the SST operator of the signal under consideration, $T^g_{s_1(t)}(t,\omega)$ we obtain the ridge map in Fig. 6. To iterate, the the signal $s_1(t)$ has three modes which are well separated in the time-frequency plane. The ridge extraction algorithm does a good job in estimating the ridges. To measure the accuracy of the ridge estimation we reconstruct the signal based on 16. The mean squared error is of the order $\mathcal{O}(10^{-4})$ for the signal $s_1(t)$.

Now we consider the signal in Section 4.2. This signal has closely packed modes in the time-frequency plane. The ridges are extracted following the same procedure. Using the same window parameters and a reduced time-frequency support because of the modes being close we perform the signal reconstruction. The mean squared error for the reconstruction of $s_2(t)$ is 0.37. There is a high error in reconstruction of the modes. This gives us a very important result that the ridge estimation and the mode recovery does not perform very well for closely packed modes. As Flandrin mentions in [4], the frequency bandwidth of the gaussian window chosen should satisfy 8. In this case, this inequality is violated and hence results in reconstruction with significant error. Therefore, there is need to shift our focus on a making the SST more adaptive in nature.

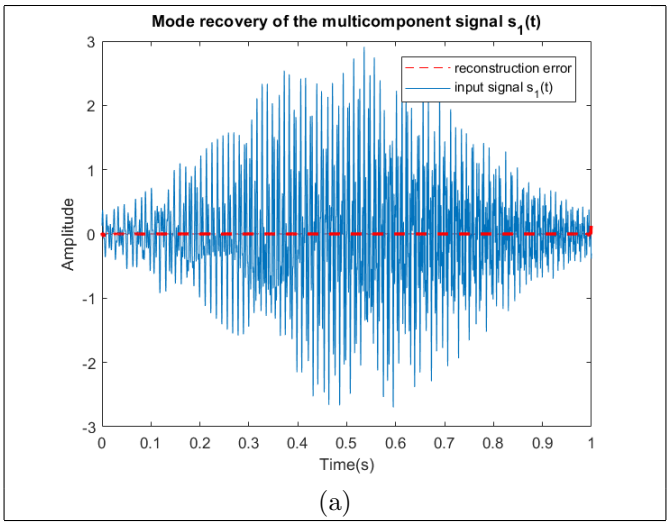

(a)

Figure 9: he input signal $s_1(t)$ and its reconstruction error is shown. The signal was reconstructed perfectly because of the well separation of the modes in TF plane.

Now that we have established certain limitations of the SST in reference to the window parameters defined earlier. we consider a bat signal from MATLAB. It consists of four distinct hyperbolic chirps. The low frequency hyperbolic chirps have the maximum energy of the signal. The spectrogram of the bat signal in Fig. 5 shows very poor resolution along the time and the frequency axis. The SST shows the chirps clearly localized in the TF plane. The ridges are then extracted and the modes are recovered following the same procedure. Since the modes are well separated a large time frequency support can be used to recover the signal back. Fig. 11 shows the error of the signal against the input signal.

8 Team members contribution

The tasks were divided into two categories namely, implementation of the synchrosqueezing transform and the mode recovery from ridge extraction. Researcher 1 carried out the literature review of the synchrosqueezing transform, involved in the discussion of making the SST adaptive. Researcher 2 was a part of the literature review of SST and carried out the literature review of the ridge extraction and the mode recovery. Researcher 2 developed an initial version of the algorithm for an adaptive time-frequency support. Researchers 1 and 2 were equally involved in developing the code for computing the SST, ridge extraction and mode recovery.

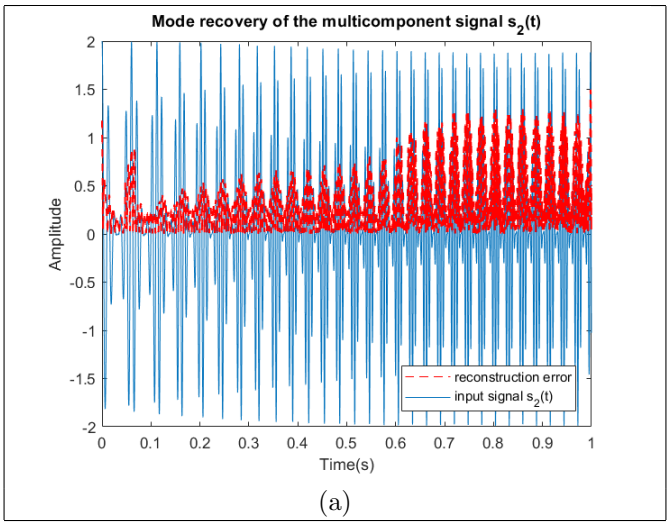

Figure 10: The input signal $s_2(t)$ and its reconstruction error is shown. It shows significant error because of the separation of modes does not satisfy the frequency bandwidth criteria in equation 8.

9 Conclusion

From the above discussion, we can say that the SST has takes into consideration quite a few parameters. To name a few the window length, the standard deviation of the window and the time frequency support. The researchers would like to point out that the the SST provides a clear time-frequency representation that shows the mode separation however, the ridge extraction is inhibited by various mathematical assumptions. We can say that there is a future scope in making the SST more adaptive in nature. One possible way to make it adaptive is to have a variable time-frequency support which will be discussed to some extent in Section 9.1. From the conclusions above one can see that in terms of closely packed modes the SST operator incurred significant amount of error. To over come this a better estimate of the ridges and the centroid calculations can be done. Recently significant amount of research is being carried out to extend the basic SST to higher order SST. Higher order implies estimating the centroid using higher order derivatives of the STFT. The researchers at this point will not delve deeper into this concept but however would like to refer the reader to the work on higher order SST carried out in [12].

9.1 Adaptive time-frequency support

The initial idea of the adaptive TFR is to make the time-frequency support variable. Consider the signal $s_1(t)$, where there are three modes. Given a constant time-frequency support derived from the window parameters, it may not hold always if the ridges are very close to each other. If we go by the approach of a constant time-frequency support and the ridges are close to each other, while reconstructing each mode

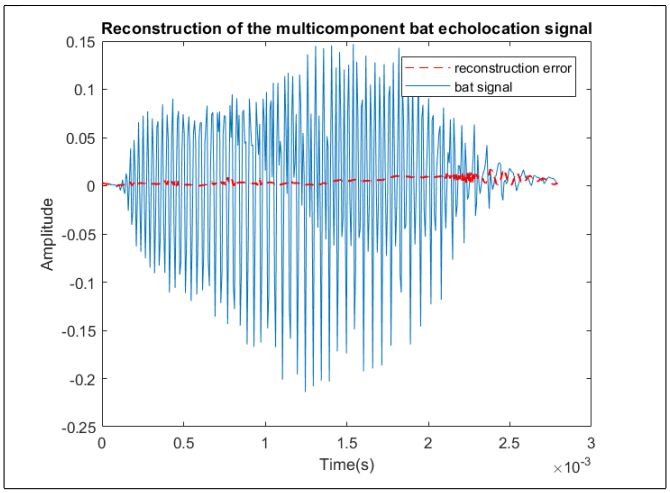

Figure 11: The input signal (bat signal) is compared against the reconstruction error. The reconstruction error is small which implies that the accuracy of the signal reconstruction is good. The number of the frequency bins selected to form the time-frequency support is 70.

the components of the neighboring ridges will be used to reconstruct the current mode. This induces error which is unnecessary. Instead to avoid this error one can form a more adaptive time frequency support by taking into account of the positions of the ridges around the current ridge which is being reconstructed.

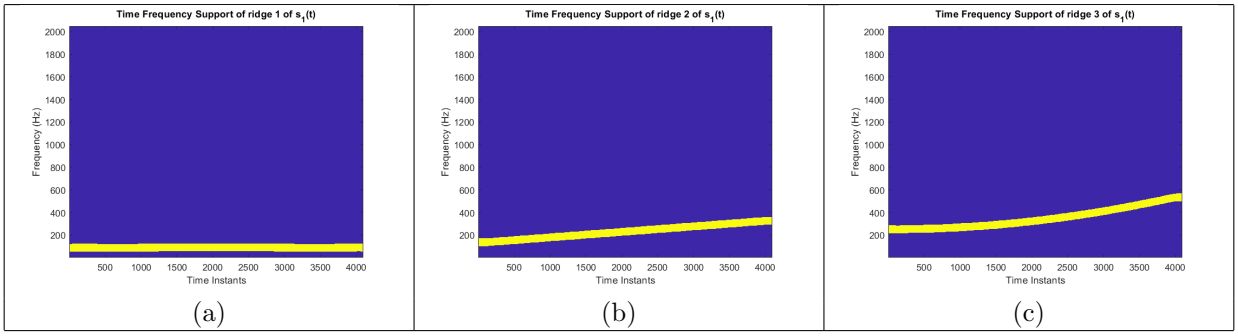

Figure 12: Masks of a constant time-frequency support around the estimated ridges of $s_1(t)$.The number of frequency bins around each ridge is 34. (a)time-frequency support mask around ridge 1(b)time-frequency support mask around ridge 2(c)time-frequency support mask around ridge 3

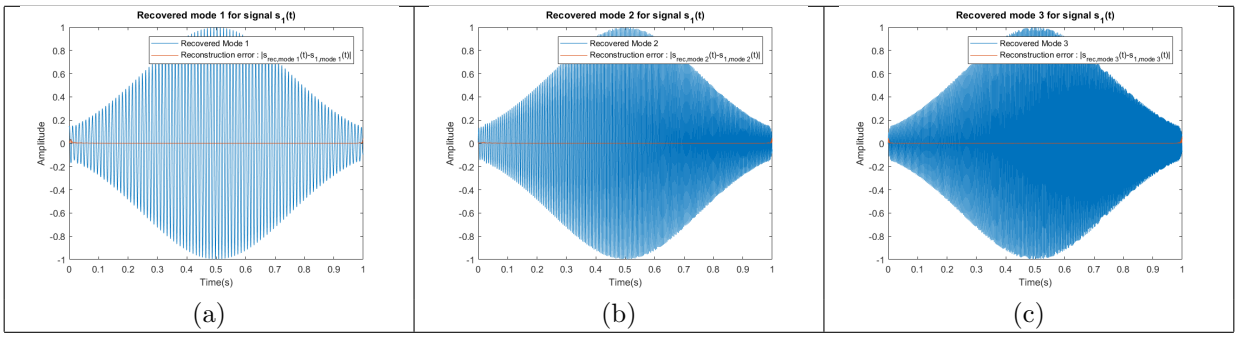

Figure 13: Individual mode recovery from the SST of $s_1(t)$.The number of frequency bins around each ridge to reconstruct the signal is 34. Using the time-frequency support displayed in Fig.12 for each mode the reconstruction was carried out using the equation 16 (a) reconstructed mode 1 and the reconstruction error (b) reconstructed mode 2 and the reconstruction error (c) reconstructed mode 3 and the reconstruction error

References

[1] A. Papandreou-Suppappola, "Applications in time-frequency signal processing", *Electrical engineering and applied signal processing series*, London, CRC Press, 2003.

[2] L. Cohen, "Time-frequency analysis", Englewood Cliffs, N.J: Prentice Hall PTR, 1995.

[3] I. Daubechies and S. Maes, "A non-linear squeezing of the continuous wavelet transform based on auditory nerve models," *Wavelets Med. Biol.*, pp. 527-546, 1996.

[4] F. Auger, P. Flandrin, Y. Lin, S. McLaughlin, S. Meignen, T. Oberlin and H. Wu, "Time-Frequency Reassignment and Synchrosqueezing: An Overview," *IEEE Signal Processing Magazine*, vol. 30, no. 6, pp. 31-42, 2013.

[5] T. Oberlin, S. Meignen and V. Perrier, "The Fourier Based Synchrosqueezing Transform," *IEEE International Conference on Acoustics, Speech and Signal Processing (ICASSP)*, pp. 315-319, 2014.

[6] J. Thakur and H.-T. Wu, "Synchrosqueezing based recovery of instantaneous frequency from nonuniform samples," *SIAM J. Math. Anal.*, vol. 43, no. 5, pp. 2078-2095, 2011.

[7] R. A. Carmona, W. L. Hwang, and B. Torresani, "Multiridge detection and time-frequency reconstruction," *IEEE Trans. Signal Processing*, vol. 47, no. 2, pp. 480-492, 1999.

[8] R. A. Carmona, W. L. Hwang and B. Torresani, 'Characterization of signals by the ridges of their wavelet transforms', *IEEE Transactions on Signal Processing*, vol. 45, no. 10, pp. 2586-2590, 1997.

[9] C. Li, M. Liang, "Time frequency signal analysis for gearbox fault diagnosis using a generalized synchrosqueezing transform", *Mechanical Systems and Signal Processing*, Vol. 26, pp. 205-217, 2012.

[10] Matlab codes used in the exprimentation can be found at:
http://www-ljk.imag.fr/membres/Thomas.Oberlin/ic14.tar.gz

[11] D. Iatsenko, P. V.E. McClintock and A. Stefanovska, "Linear and synchrosqueezed timefrequency representations revisited: Overview, standards of use, resolution, reconstruction, concentration, and algorithms", *Digital Signal Processing*, vol. 42, pp. 1-26, 2015.

[12] D. Pham and S. Meignen, "High-Order Synchrosqueezing Transform for Multicomponent Signals AnalysisWith an Application to Gravitational-Wave Signal", *IEEE Transactions on Signal Processing*, vol. 65, pp. 3168-3178, 2017.